Role of Dimensionality and Axisymmetry in Fluid Pinch-Off and Coalescence

J. C. Burton and P. Taborek

Department of Physics and Astronomy, University of California, Irvine, California, USA

(Received 21 July 2006; published 29 May 2007)

We present data on the pinch-off and coalescence of thin liquid alkane lenses floating on water. Pinch-off in quasi-2D lenses is distinctly different from pinch-off in axisymmetric 3D drops and involves a cascade of satellite droplets which extends to micron length scales. In contrast, coalescence of lenses is qualitatively similar to coalescence of 3D drops. Coalescence is predicted to involve entrainment of the exterior fluid as the droplets merge. This reentrant folding is obscured in 3D droplets but is clearly visible in coalescence of thin lenses.

DOI: 10.1103/PhysRevLett.98.224502 PACS numbers: 47.20.Dr, 47.55.df, 47.55.nd

The breakup and coalescence of droplets and bubbles are simple examples of systems in which dynamics leads to a change in topology. In some cases, the singularities at pinch-off or coalescence can be described by power laws that are universal, but recently it has become clear that this is not always the case [1–3]. A complete analysis of the possible types of singularities is not yet available, but dimensionality is thought to play an important role [4–6]. Most experiments and theory on 3D pinch-off and coalescence involve axisymmetric drops or bubbles. However, recent experiments show that breaking this symmetry can significantly alter the asymptotic dynamics [3,7]. Pinch-off and coalescence both involve a conversion of interfacial energy into kinetic energy of flow. At the singular point, the interfacial curvature, pressure, and fluid velocity all diverge. These topology-changing transformations are important for practical issues such as emulsification, mixing [8], and formation of sprays and foams, and also because they are a model system for the intrinsically nonlinear fission and fusion processes which occur in a wide variety of contexts from biology to astrophysics. The goals of the experiments reported in this Letter are to investigate the effects of reduced dimension and loss of axisymmetry on flow singularities using quasi-2D liquid lenses as a test system.

In 3D, the interfacial energy which drives the flow is described by a surface tension σ, while in 2D the interfacial energy is described by a line tension. For the intermediate case of thin liquid lenses on water (similar to the drops of fat in chicken soup), the energetics are described by a spreading coefficient $S = \sigma_{wa} - \sigma_{wo} - \sigma_{oa}$, where the subscripts denote the water-air, water-oil, and oil-air interfaces, respectively. The spreading coefficient is usually much smaller than the surface tensions of the individual fluids, so that characteristic velocities in liquid lens systems are less than their 3D axisymmetric droplet counterparts. For all of the alkanes used in our experiments, S is negative, so the oil meets the water at a three-phase contact line at a finite contact angle, which is 14° for an octane lens, 36° for decane, and 46° for dodecane, as calculated from formulas in Ref. [9]. For small drops of oil, gravity is negligible, and the lenses have a spherical cap shape. Larger volumes of oil form "pancake"-shaped lenses whose thickness h is given by $h^2 = -2S\rho_w/[g\rho_o(\rho_w - \rho_o)]$ [9], where ρ_x is the density of the oil or water, and g is the acceleration due to gravity. The volumes of the lenses in the experiments were initially near the pancake limit, but smaller satellite lenses were spherical caps. Both the alkanes and the underlying water are simple Newtonian fluids with very low viscosity ($\eta \sim 1$ cP).

The experimental apparatus consisted of a glass trough of adjustable width (0–25 mm) mounted to the stage of a microscope, equipped with long focal distance objectives. A Phantom V7.2 video camera with a maximum frame rate of 200 000 fps was mounted vertically on the top of the microscope. Both the lenses and the water are transparent, so the optical contrast comes from variations in curvature near the edges of the lens. Fluids used in the experiment consisted of pure n-dodecane, n-decane, and n-octane obtained from Aldrich. Data for viscosities, densities, and spreading coefficients were taken from Refs. [10,11]. The water formed a shallow meniscus in the trough which kept the lenses centered and prevented them from wicking onto the glass walls of the trough. Initiating pinch-off requires a method of breaking the rotational symmetry and forcing the droplet into a metastable elongated shape. Gravity does not elongate liquid lenses, so we used two techniques to initiate deformation. The first involves pulling apart a single lens in quiescent water using preferential wetting of alkanes on metal probes inserted into the drop. The second method utilizes a flow rate in the underlying water to deform a lens wicked onto the end of a capillary. Using a flowing trough has the experimental advantage of reproducibly localizing the pinch-off at the imaging plane of the microscope and keeping the underlying water clean and free of surface contaminants, so most of our experiments were done in this way. The flow velocity of the underlying water was ≤ 0.5 cm/s. The typical initial radius of the lens R was 3.5 mm. The flow rate has only a minor effect on the pinch-off process, as indicated qualitatively by the symmetric hourglass shape of the lenses before pinching and quantitatively by the fact that the Weber number con-

 © 2007 The American Physical Society

structed from the spreading coefficient and the trough flow velocity is always less than 0.1. This was confirmed by experiments in quiescent water, which showed identical pinch-off phenomena.

Once the lens has been elongated beyond a threshold value, pinch-off proceeds spontaneously. The central region of the fluid filament connecting the separating lenses widens and forms two daughter filaments, which in turn form a wider central region and another generation of daughter filaments. This process continues for up to 5 generations, resulting in $\sim 2^5$ visible satellite lenses which form as the wider sections pinch off from the filaments. The largest central satellite lens is of the order of 500 μm in diameter, and the smallest satellite lenses are of the order of 3 μm in diameter. Each generation of satellite lenses is smaller than the last by approximately a factor of 3. This hierarchical process is distinctly different from pinch-off in 3D axisymmetric drops, as illustrated in Fig. 1, which compares pinch-off of a 3D decane drop surrounded by water with pinch-off of a quasi-2D decane lens at the same optical magnification. The 3D droplet shows the asymmetrical cone-shaped contact typical of inviscid pinch-off; this cone-shaped filament retracts with an approximately constant angle and eventually forms a single satellite droplet. The filaments of the decane lens, in contrast, have a complicated time-varying structure which produces many satellite droplets with more than 2 orders of magnitude variation in length scales (3–500 μm). The time evolution of the filament structures is illustrated in the vertical sequence of video frames in Fig. 2. This cascade proceeds down to our optical resolution of 2.2 μm per pixel. Despite the variation in the contact angle and initial thickness of the lenses, the pinch-off cascade is a robust feature observed for all alkanes used in the experiment.

Typical analysis [12] of 3D pinch-off is focused on determination of the exponent n in the relation $r_{\min} \propto \tau^n$, where $r_{\min}$ is the minimum neck radius and τ is the time before pinch-off. In the case of liquid lenses, this type of analysis is not practical, because the location of the minimum neck radius is not a continuous function of time; local minima often evolve into local maxima and mark the location of the center of a satellite drop rather than a pinch. The numerous pinch events that arise also complicate the definition of τ. Pinch-off scenarios that involve multiple generations of satellite droplets have been observed previously in polymer solutions [13] and high viscosity fluids [14] pinching in air and also in simulations of surfactant solutions [15]. Pinch-off cascades superficially similar to those in Fig. 2 are observed in the Stokes flow relaxation of highly elongated 3D drops suspended in an exterior high viscosity fluid of equal density [16], although the fluid properties are strikingly different [17]. We are not aware

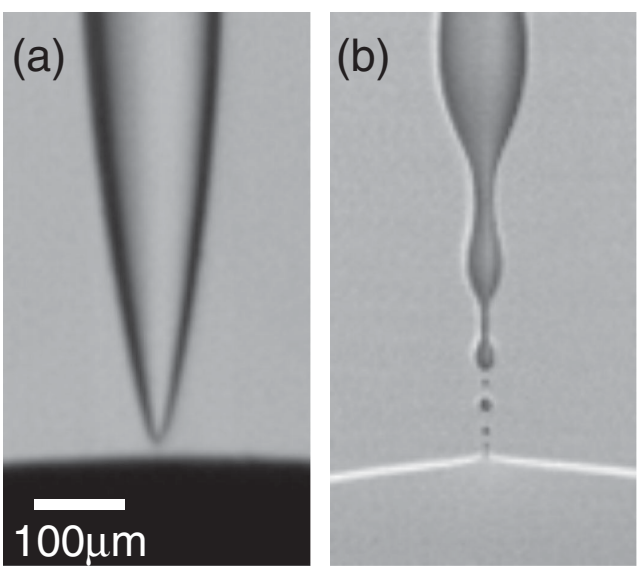

FIG. 1. (a) Breakup of a 3D decane droplet immersed in water just after pinch-off. Both the cone-shaped structure and the dark region at the bottom are decane. The neck has a well-defined angle and rounded tip characteristic of inviscid pinch-off [24]. (b) Breakup of a quasi-2D decane lens on the surface of water just after pinch-off at the same magnification as (a). A cascade of pinch-off events creates multiple satellite droplets in a fractal-like structure. The bottom of the image is the large lens shown in the right-hand edge of the images in Fig. 2.

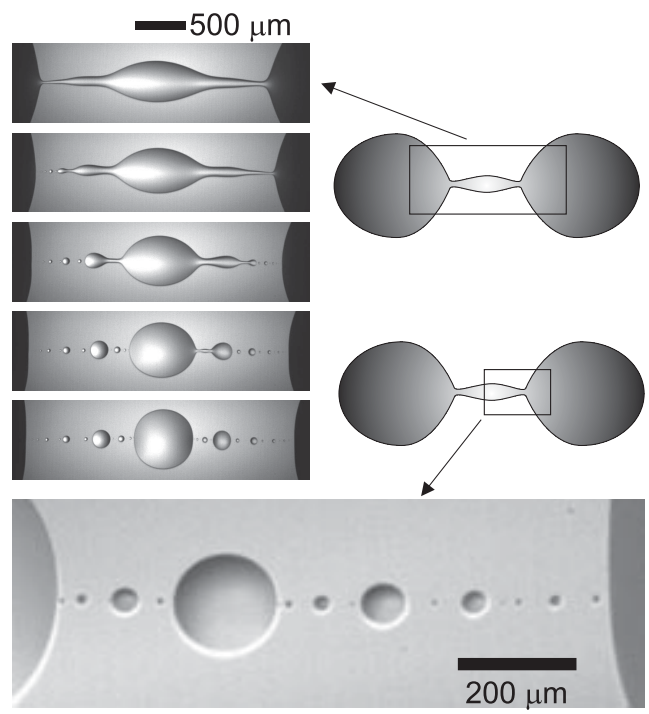

FIG. 2. Video frames of the breakup of a decane lens illuminated from below. Magnification is indicated by the bars. The vertical sequence shows the central region of the filament as it undergoes a cascade of pinches. The time interval between frames is 748 μs. The high magnification image just below the sequence shows just the right half of this filament immediately after breakup, which displays a complex structure of the remaining satellite lenses. Multiple satellite lenses are formed in a range of sizes which extends to below our optical resolution of 2.2 μm per pixel.

of a simple common feature shared by these diverse systems which can account for the complex cascade of pinch-offs in a general way. To our knowledge, cascade pinch-off of liquid alkane lenses is the first example of this behavior in a low viscosity simple fluid system.

We turn now to coalescence, which we studied by bringing two initially circular lenses together in quiescent water. High speed video images of the coalescence event were imported into MATHEMATICA for edge-tracking analysis. Figure 3(a) shows the coalescence of dodecane lenses which have a 46° contact angle and are, therefore, relatively thick. The neck region which grows as coalescence proceeds has lower curvature and appears light in the photographs. Coalescence of conventional 3D drops has recently been studied both theoretically [18,19] and experimentally [20–23]. These studies have shown that, for 3D drops, the characteristic minimum radius of the connecting neck should scale as $r_{\min} \propto (\sigma R/\rho)^{1/4}\tau^{1/2}$ in the inviscid limit [18,19], where R is the initial radius of the drop, and τ is the time elapsed after the moment of initial connection. At short times when viscous forces are expected to dominate the flow, the scaling is linear, with $r_{\min} \sim \sigma\tau/(4\pi\eta)$, with logarithmic corrections. The factor of 4π is present when the drop is immersed in a quiescent fluid of equal viscosity [19]. We expect that this formula will provide a reliable estimate for lenses as well, since the theoretical predictions for 3D and 2D drops are essentially the same [19].

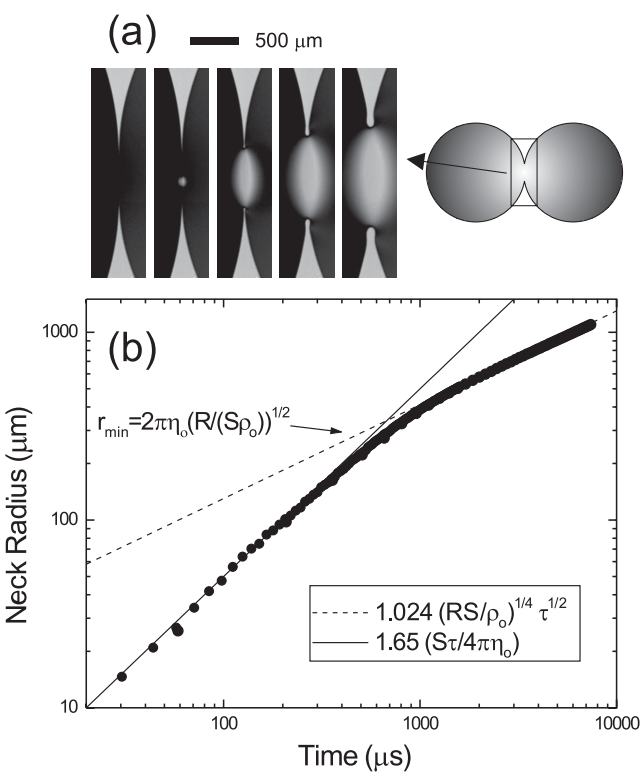

FIG. 3. (a) Coalescence of two dodecane lenses. The curvature of a dodecane lens is large enough to scatter the light and appear dark. At the moment of connection, a light spot appears, indicating that the curvature is flattened as the two lenses merge together. The time interval between frames is 748 μs. (b) Log-log plot of the minimum radius ($r_{\min}$) of the connecting necks between two dodecane lenses during coalescence versus the time elapsed from the initial connection (τ). The change in slope signifies a transition between inertial-capillary ($r_{\min} \propto \tau^{1/2}$) and viscous-capillary scaling ($r_{\min} \propto \tau$), as indicated by the dashed and solid lines, respectively. The crossover length l_c is indicated by the arrow. Note that the coefficients of the scaling forms are of the order of 1.

A log-log plot of $r_{\min}$ as a function of τ obtained from videos of dodecane lens coalescence is shown in Fig. 3(b). The data show regions where $r_{\min} \propto \tau$ and regions where $r_{\min} \propto \tau^{1/2}$, with a smooth transition region between them. Previous viscous-inertial transitions have been observed in the coalescence of 3D axisymmetric drops [20,21], with a crossover in behavior when $r_{\min}$ exceeds the natural viscous length scale $\eta^2/(\sigma\rho)$. In contrast, the crossover length that we observe in liquid lenses ($\sim$250 μm) is several orders of magnitude larger than the natural viscous length scale for our system $\eta_o^2/(S\rho_o)$, which is approximately 0.5 μm for alkanes on water. However, we note that a reasonable estimate for the crossover length can be obtained by replacing parameters in the theory for 3D axisymmetric coalescence with appropriate values in the liquid lens system. The resulting proportionalities are $r_{\min} \propto (SR/\rho_o)^{1/4}\tau^{1/2}$ in the inviscid regime and $r_{\min} \sim S\tau/(4\pi\eta_o)$ in the viscous regime. Since the transition between the two regimes is smooth, a crossover length l_c can be obtained by equating velocities from the two scaling laws $l_c \simeq 2\pi\eta_o\sqrt{R/(\sigma\rho_o)}$. In the dodecane lens system, $l_c = 253$ μm, which is in good agreement with the observed crossover region from Fig. 3(b). This crossover was observed in both spherical cap and pancake-shaped lenses.

Detailed calculations of coalescence of both inviscid [18] and viscous [19] drops predict that, in addition to the power law growth of $r_{\min}$ with τ, complicated structures are generated near the cusps of the merging droplets due to entrainment and subsequent pinch-off of regions of the exterior fluid. For 3D drops coalescing in air, this is expected to lead to the formation of toroidal bubbles, but this effect has not been experimentally verified because of the difficulty of imaging inside the liquid drop. The analogous phenomenon in lens coalescence is the entrainment of air or water within the merging alkane lens which can be observed from above. Figure 4 shows a sequence of video frames of the coalescence of octane lenses. The dark features are high curvature regions near the contact lines. The video shows the formation of holes in the alkane lens near the initial contact point. The holes merge into a single hole, which eventually collapses and disappears. The end points of the neck have a teardrop shape which is similar to shapes calculated for coalescence of a viscous droplet in the presence of an exterior fluid with finite viscosity [19]. It is interesting to note that, although all alkanes used in the experiment displayed a crossover in the scaling behavior of

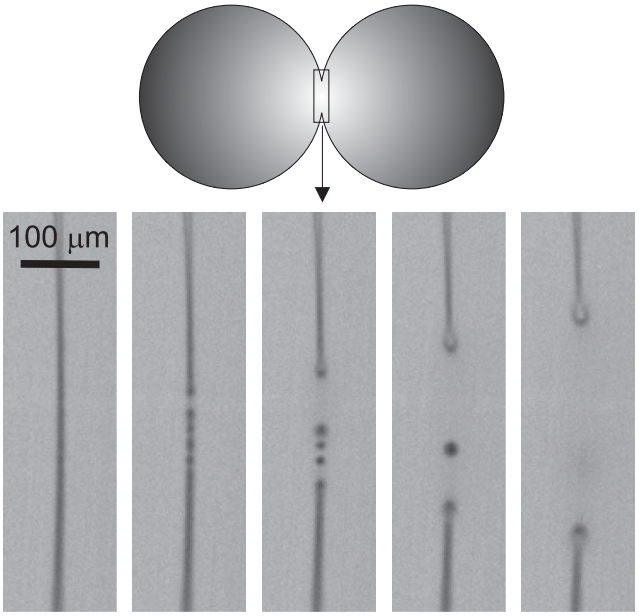

FIG. 4. High magnification images of the coalescence of two octane lenses. The dark line is the three-phase air-water-octane contact line. The initial coalescence event triggers an instability which results in multiple holes that become trapped in the film and then eventually disappear when the alkane closes around them. The time interval between frames is 180 μs.

$r_{\min}$ as a function of τ as shown in Fig. 3, only octane lenses generated entrained holes as shown in Fig. 4. We suspect that the reason for this is that the energetic cost of the formation of the holes is proportional to the lens thickness, which is determined by the contact angle. The octane lenses are considerably thinner than the other alkanes and provide a smaller energy barrier for the nucleation of holes.

In conclusion, our experiments suggest that reduced dimensionality and symmetry qualitatively alter the dynamics of fluid pinch-off but have relatively little effect on the dynamics of coalescence. Pinch-off in alkane lenses spontaneously generates a complex pattern with length scales spanning almost 3 orders of magnitude. Coalescence of lenses is qualitatively similar to the predictions for coalescence of 3D spherical drops. The dynamics is described by power laws with a transition from viscous to inviscid behavior, which occurs, however, at a length scale more than 2 orders of magnitude larger than the natural viscous length scale. In thin lenses, an instability in the boundary traps holes in the film which survive for $\sim$200 μs before coalescing with other holes or collapsing. The liquid lens system has a rich and diverse phase space of fluid parameters to explore such as viscosity of the liquids, flow velocity of the subphase, and three dynamic contact angles, which we hope to address in future work.

This work was supported by NSF Grant No. DMR 0509685.

[1] P. Doshi, I. Cohen, W. Zhang, M. Siegel, P. Howell, and O. Basaran, Science **302**, 1185 (2003).
[2] J. C. Burton, R. Waldrep, and P. Taborek, Phys. Rev. Lett. **94**, 184502 (2005).
[3] N. C. Keim, P. Moller, W. W. Zhang, and S. R. Nagel, Phys. Rev. Lett. **97**, 144503 (2006).
[4] P. Constantin, T. F. Dupont, R. E. Goldstein, L. P. Kadano, M. J. Shelly, and S. Zhou, Phys. Rev. E **47**, 4169 (1993).
[5] D. Vaynblat, J. R. Lister, and T. P. Witelski, Eur. J. Appl. Math. **12**, 209 (2001).
[6] J. B. Keller, A. P. Milewski, and J. Vanden-Broeck, J. Eng. Math. **42**, 283 (2002).
[7] W. D. Ristenpart, P. M. McCalla, R. V. Roy, and H. A. Stone, Phys. Rev. Lett. **97**, 064501 (2006).
[8] J. M. Shaw, Spill Sci. Technol. Bull. **8**, 491 (2003).
[9] I. Langmuir, J. Chem. Phys. **1**, 756 (1933).
[10] *CRC Handbook of Chemistry and Physics*, edited by D. R. Lide (CRC Press, Boca Raton, FL, 2006), 86th ed.
[11] S. Zeppieri, J. Rodriguez, and A. L. L. de Ramos, J. Chem. Eng. Data **46**, 1086 (2001).
[12] J. C. Burton, J. E. Rutledge, and P. Taborek, Phys. Rev. Lett. **92**, 244505 (2004).
[13] M. S. N. Oliveira and G. H. McKinley, Phys. Fluids **17**, 071704 (2005).
[14] X. D. Shi, M. P. Brenner, and S. R. Nagel, Science **265**, 219 (1994).
[15] P. T. McGough and O. A. Basaran, Phys. Rev. Lett. **96**, 054502 (2006).
[16] M. Tjahjadi, H. A. Stone, and J. M. Ottino, J. Fluid Mech. **243**, 297 (1992).
[17] The flow structures described in both this Letter and Ref. [16] range from millimeters to microns. In pinch-off, flows with length scales less than a characteristic value of $\eta^2/\rho\sigma$ are dominated by effects of viscosity. For the fluids used in Ref. [16], this length scale is of the order of 50 cm. Thus, experiments in Ref. [16] are clearly in the Stokes flow limit, as confirmed by their analysis. For alkane liquid lenses, this formula must be modified by the replacement of σ with S. The resulting expression is $\eta^2/\rho S$, which is approximately 0.5 μm for all fluids used in our experiments. This indicates that these experiments are in different flow regimes.
[18] L. Duchemin, J. Eggers, and C. Josserand, J. Fluid Mech. **487**, 167 (2003).
[19] J. Eggers, J. R. Lister, and H. A. Stone, J. Fluid Mech. **401**, 293 (1999).
[20] D. G. A. L. Aarts, H. N. W. Lekkerkerker, H. Guo, G. H. Wegdam, and D. Bonn, Phys. Rev. Lett. **95**, 164503 (2005).
[21] S. T. Thoroddsen, K. Takehara, and T. G. Etoh, J. Fluid Mech. **527**, 85 (2005).
[22] A. Menchaca-Rocha, A. Martnez-Davalos, R. Nunez, S. Popinet, and S. Zaleski, Phys. Rev. E **63**, 046309 (2001).
[23] S. G. Bradley and C. D. Stow, Phil. Trans. R. Soc. A **287**, 635 (1978).
[24] M. Nitsche and P. H. Steen, J. Comput. Phys. **200**, 299 (2004).